MULTI-STREAM TRANSMISSION IN MIMO-FBMC SYSTEMS

Màrius Caus[1] *and Ana I. Pérez-Neira*[1,2]

[1]Dept. of Signal Theory and Communications - Universitat Politècnica de Catalunya (UPC)
[2]Centre Tecnològic de Telecomunicacions de Catalunya (CTTC)

ABSTRACT

This paper addresses the design of MIMO precoding and decoding techniques for the filter bank multicarrier (FBMC) modulation. Existing solutions give satisfactory performance in scenarios with high coherence bandwidth channels. With the aim of increasing the robustness against the channel frequency selectivity, we have rethought the problem, which results in a new subband processing. Simulation-based results show that the proposed solution can achieve similar bit error rates as the OFDM solution, while the spectral efficiency is increased. These results are theoretically justified. As a conclusion, FBMC becomes attractive in frequency selective channels not only because it relaxes the frame synchronization with respect to OFDM, but also because it presents spatial multiplexing competitive results.

Index Terms— FBMC, OFDM, MIMO precoder/decoder

1. INTRODUCTION

Multiple-input-multiple-output (MIMO) techniques are able to boost the system performance without the necessity of using additional bandwidth. The MIMO techniques are usually combined with multicarrier modulations (MCMs) to lower the dispersion of the channel. In this sense, the orthogonal frequency division multiplexing (OFDM) is the favourite MCM since the fading at the subcarrier level is modeled flat, which facilitates the implementation of the MIMO concept. However the OFDM performance relies on transmitting redundancy in the form of a cyclic prefix (CP), which has to be larger than the maximum channel excess delay.

It is worth mentioning that OFDM presents several drawbacks since the subcarrier signals do not present good frequency localization. In this sense, the filter bank multicarrier (FBMC) modulation may become a candidate to overcome some of the OFDM limitations [1, 2]. The conclusion is that for some system parameters and scenarios, FBMC should be the first choice. For instance, FBMC is preferred to OFDM if the transmitter and the receiver are unlikely to be tightly synchronized. This highlights that the comparison between OFDM and FBMC is sometimes difficult, since they might be designed to meet different goals.

In this paper, we study how to combine MIMO techniques with the FBMC modulation. To the best of authors' knowledge the approach followed in [3], which represents one of the few works that study multi-stream transmission in MIMO-FBMC systems, is valid for high coherence bandwidth channels. With the aim of making the FBMC system more robust against the channel frequency selectivity we propose a novel solution, which is based on concatenating two precoding matrices. We first design one of the precoders to cancel the interferences induced by the channel. In the second step, the receive filters and the remaining precoders are jointly designed so that the sum mean square error (MSE) is minimized. It must be mentioned that the work in [4] also investigates the design of MIMO-FBMC systems. The solution devised in [4] does not make any assumption about the flatness of the channel, thus it gives satisfactory performance for low coherence bandwidth channels, but the technique is only able to multiplex a single stream per-subband for a fixed power allocation. The technique presented in this paper represents an improvement since it supports multi-stream transmission while it offers some degree of resilience against the channel frequency selectivity. In addition, the numerical results confirm that the proposed solution remains competitive with OFDM in some cases.

In Section 2 we define the expressions that are involved in a MIMO-FBMC system. The proposed solution is described in Section 3. Next we conduct simulations in Section 4 to evaluate the novel technique. Finally, the conclusions are drawn in Section 5.

2. MIMO-FBMC SYSTEM MODEL

Consider a multi-stream transmission over a $N_R \times N_T$ MIMO communication system where the transmitter and the receiver are equipped with N_T and N_R antennas, respectively. To combat the channel frequency selectivity, the band is partitioned into *M* subchannels by implementing the FBMC modulation scheme [1]. If the channel state information is available at the transmitter, the streams to be spatially multiplexed

The research leading to these results has received funding from the Spanish Ministry of Science and Innovation under projects TEC2011-29006-C03-02 (GRE3N-LINK-MAC) and the Catalan Government (2009SGR0891). This work is also partially supported by the European project EMPhAtiC (ICT- 318362).

Table 1. Intrinsic interferences under ideal propagation conditions

	k=-3	k=-2	k=-1	k=0	k=1	k=2	k=3
m=q-1	-j0.0429	-0.1250	j0.2058	0.2393	-j0.2058	-0.1250	j0.0429
m=q	-0.0668	0	0.5644	1	0.5644	0	-0.0668
m=q+1	j0.0429	-0.1250	-j0.2058	0.2393	j0.2058	-0.1250	-j0.0429

on subband *m* can be linearly precoded as follows $\mathbf{v}_m[k] = \mathbf{B}_m\mathbf{x}_m[k]$, where $\mathbf{v}_m[k] \in \mathbb{C}^{N_T\times 1}$ is the vector of precoded symbols and $\mathbf{B}_m \in \mathbb{C}^{N_T\times S}$ is the linear precoder. We assume that *S* streams are simultaneously transmitted on each subband. Then the vector of symbols that is transmitted on the *m*th subband and *k*th time instant is given by $\mathbf{x}_m[k] = \theta_m[k]\mathbf{d}_m[k] = \theta_m[k]\left[d_m^1[k]...d_m^S[k]\right]^T$. Since the symbols must be drawn from the offset QAM (OQAM) [1], we can factorize $\mathbf{x}_m[k]$ as the product of a vector that contains real PAM symbols and a phase term, which is defined as

$$\theta_m[k] = \left\{ \begin{array}{cc} 1 & m+k \;\; even \\ j & m+k \;\; odd \end{array} \right\}. \quad (1)$$

The transmission of OQAM symbols enables us to use pulse shaping techniques [1]. Bearing this in mind, the baseband signal transmitted by the *i*th antenna can be expressed as

$$s_i[n] = \sum_{k=-\infty}^{\infty}\sum_{m=0}^{M-1} v_m^i[k] f_m\left[n - k\frac{M}{2}\right] \quad (2)$$

$$f_m[n] = p[n]e^{j\frac{2\pi}{M}m\left(n-\frac{L-1}{2}\right)}. \quad (3)$$

Here $v_m^i[k]$ denotes the *i*th element of $\mathbf{v}_m[k]$. The pulse $p[n]$ is designed according to [5] with a length equal to $L = 4M$. For the sake of clarity the low-rate signals use the sampling index *k* while the high-rate signals utilize the index *n*.

Let $h_{ij}[n]$ be the channel that impairs the reception of the *j*th receive antenna when the signal comes from the *i*th transmit antenna. Then it follows that the samples received by the *j*th antenna reads as $r_j[n] = \sum_{i=1}^{N_T} s_i[n] * h_{ij}[n] + w_j[n]$. In addition, the signal is contaminated by additive noise. At this point, each receiver chain operates on a block-by-block fashion to demodulate the signals. This implies that the samples are fed into a bank of filters and next the outputs are downsampled, yielding $z_q^j[k] = \left(r_j[n] * f_q^*[-n]\right)_{\downarrow\frac{M}{2}}$ for $0 \le q \le M-1$. The expression $(.)_{\downarrow x}$ accounts for a decimation by a factor of *x*. The signal $z_q^j[k]$ can be compactly written as

$$z_q^j[k] = \sum_{m=q-1}^{q+1}\sum_{i=1}^{N_T} v_m^i[k] * g_{qm}^{ij}[k] + w_q^j[k] \quad (4)$$

$$g_{qm}^{ij}[k] = \left(f_m[n] * h_{ij}[n] * f_q^*[-n]\right)_{\downarrow\frac{M}{2}} \approx H_j^i(m)\alpha_{qm}[k]. \quad (5)$$

The filtered noise in the *q*th subband is expressed as $w_q^j[k] = \left(w_j[n] * f_q^*[-n]\right)_{\downarrow\frac{M}{2}}$. Thanks to the good spectral confinement of the pulses, the inter-carrier interference (ICI) only comes from the adjacent subbands. The approximation in (5) is consequence of assuming that the channel frequency response (CFR) is flat at the subcarrier level. In notation terms, $H_j^i(m)$ denotes the CFR of $h_{ij}[n]$ on the frequency $\frac{2\pi}{M}m$ and $\alpha_{qm}[k]$ represents the intrinsic interference term, which is defined as $\alpha_{qm}[k] = \left(f_m[n] * f_q^*[-n]\right)_{\downarrow\frac{M}{2}}$. As Table 1 indicates, $\alpha_{qm}[k]$ only takes significant values in a small neighborhood around the position of interest. The values in Table 1 correspond to the case that *q* is even. For *q* odd, the magnitudes keep unchanged and only differ in the signs.

Arranging the terms as follows $\mathbf{z}_q[k] = \left[z_q^1[k]...z_q^{N_R}[k]\right]^T$, the equalized signals can be expressed as $\mathbf{y}_q[k] = \mathbf{A}_q^T\mathbf{z}_q[k]$, where $\mathbf{A}_q \in \mathbb{R}^{N_R\times S}$. Constraining the decoding matrix $\mathbf{A}_q$ to be real-valued will simplify the design as next section highlights. Finally, the symbols are detected by compensating the phase term and extracting the real component, i.e. $\check{\mathbf{d}}_q[k] = \Re\left(\theta_q^*[k]\mathbf{y}_q[k]\right)$. Expanding the vector of estimated symbols we end up with this equation

$$\begin{aligned}\check{\mathbf{d}}_q[k] = \sum_{m=q-1}^{q+1}\sum_{l=-3}^{3} \mathbf{A}_q^T\Re\left(\theta_q^*[k]\theta_m[k-l]\alpha_{qm}[l]\right. \\ \left.\times\mathbf{H}_m\mathbf{B}_m\right)\mathbf{d}_m[k-l] + \mathbf{A}_q^T\Re\left(\theta_q^*[k]\mathbf{w}_q[k]\right)\end{aligned} \quad (6)$$

$$\mathbf{H}_m = \left[\begin{array}{ccc} H_1^1(m) & ... & H_1^{N_T}(m) \\ . & . & . \\ H_{N_R}^1(m) & ... & H_{N_R}^{N_T}(m) \end{array}\right]. \quad (7)$$

It can be inferred from (6) that $\mathbf{w}_q^T[k] = \left[w_q^1[k]...w_q^{N_R}[k]\right]$. Note that the matrix $\mathbf{A}_q^T\Re\left(\mathbf{H}_q\mathbf{B}_q\right)$ establishes the input/output relationship of those symbols transmitted on the *q*th subband and the time instant of interest. It can be checked that the interferers that come from the same subband pass through an equivalent communication system that is expressed as $|\alpha_{qq}[l]|\mathbf{A}_q^T\Im\left(\mathbf{H}_q\mathbf{B}_q\right)$, for $l \neq 0$. The symbols that give rise to ICI are multiplied by this matrix $|\alpha_{qm}[l]|\mathbf{A}_q^T\Im\left(\mathbf{H}_m\mathbf{B}_m\right)$.

3. ZF-MSE BASED SUBBAND PROCESSING

In the literature we can find several schemes that enable spatial multiplexing such as: V-BLAST [6], the regularized channel inversion [7] and the Tomlinson Harashima precoder [8]. In this work we have discarded these techniques because our objective is to jointly design the MIMO precoding and decoding matrices to achieve interference-free data multiplexing. To this end, we force the product $\mathbf{H}_m\mathbf{B}_m$ to exclusively have in-phase components, which ensures that most of the interference is removed in (6). Stacking real and imaginary parts, we can express the zero forcing (ZF) condition in this form $\Im(\mathbf{H}_m\mathbf{B}_m) = \mathbf{H}_{m,e}\mathbf{B}_{m,e} = \mathbf{0}$, where $\mathbf{H}_{m,e} = [\Im(\mathbf{H}_m)\,\Re(\mathbf{H}_m)]$ and $\mathbf{B}_{m,e} = \left[\Re\left(\mathbf{B}_m^T\right)\Im\left(\mathbf{B}_m^T\right)\right]^T$. Thus, the precoders should project the input vectors onto the null subspace of $\mathbf{H}_{m,e} \in \mathbb{R}^{N_R\times 2N_T}$. Under the assumption that $2N_T > N_R$, the singular value decomposition of the extended channel matrix is given by $\mathbf{H}_{m,e} = \mathbf{U}_m[\mathbf{D}_m\mathbf{0}][\mathbf{V}_{m,1}\mathbf{V}_{m,0}]^T$, where $\mathbf{D}_m \in \mathbb{R}^{N_R\times N_R}$ is diagonal and $\mathbf{0} \in \mathbb{R}^{N_R\times 2N_T-N_R}$ is zero-valued. As a result, the columns of $\mathbf{V}_{m,0} \in \mathbb{R}^{2N_T\times 2N_T-N_R}$ span the null space of $\mathbf{H}_{m,e}$. Then, any precoder of the form $\mathbf{B}_{m,e} = \mathbf{V}_{m,0}\mathbf{Q}_m$ cancels the interferences in the real field. Note that we have freedom to design $\mathbf{Q}_m \in \mathbb{R}^{2N_T-N_R\times S}$. When the ZF condition is satisfied, (6) can be recasted as

$$\check{\mathbf{d}}_q[k] = \mathbf{A}_q^T\bar{\mathbf{H}}_q\mathbf{Q}_q\mathbf{d}_q[k] + \mathbf{A}_q^T\Re\left(\theta_q^*[k]\mathbf{w}_q[k]\right) \tag{8}$$

$$\bar{\mathbf{H}}_q = [\Re(\mathbf{H}_m)\ \ -\Im(\mathbf{H}_m)]\,\mathbf{V}_{q,0} = (\mathbf{H}_{q,e}\mathbf{P})\,\mathbf{V}_{q,0} \tag{9}$$

$$\mathbf{P} = \begin{bmatrix} 0 & -1 \\ 1 & 0 \end{bmatrix} \otimes \mathbf{I}_{N_T}, \tag{10}$$

where $\otimes$ is the Kronecker product and $\mathbf{I}_a$ is the a-dimensional identity matrix. Assuming that $\mathbb{E}\left\{\mathbf{d}_q[k]\mathbf{d}_m^H[n]\right\} = \delta_{q,m}\delta_{k,n}\mathbf{I}_S$, the remaining system is designed to minimize the sum MSE, which comes down to solve

$$\begin{aligned} &\underset{\{\mathbf{A}_q,\mathbf{Q}_q\}}{\operatorname{argmin}} \sum_{q=0}^{M-1} \mathbb{E}\left\{\left\|\check{\mathbf{d}}_q[k] - \mathbf{d}_q[k]\right\|_2^2\right\} \\ &s.t.\ \sum_{q=0}^{M-1} \mathbb{E}\left\{\left\|\mathbf{V}_{q,0}\mathbf{Q}_q\mathbf{d}_q[k]\right\|_2^2\right\} = \sum_{q=0}^{M-1} \left\|\mathbf{Q}_q\right\|_F^2 \leq P_T. \end{aligned} \tag{11}$$

The similarity of (8) to OFDM allows us to solve (11) as [9] describes. Then, (8) will present a diagonal structure.

Assuming that $w[n] \sim \mathcal{CN}(0, N_0)$, the autocorrelation matrix of the noise samples $\Re\left(\theta_q^*[k]\mathbf{w}_q[k]\right)$ is given by $\mathbf{R}_q = \frac{N_0}{2}\mathbf{I}_{N_R}$ [4]. The signal and noise statistics together with the solution of [9] bring about this signal to noise ratio (SNR)

$$\text{SNR}_q^l = \frac{p_q^l\lambda_q^l}{N_0/2},\ \ l = 1,...,S,\ \ q = 0,...,M-1 \tag{12}$$

where λ_q^l is the lth largest eigenvalue of the matrix $\bar{\mathbf{H}}_q^T\bar{\mathbf{H}}_q$ and $p_q^l = \max\left(\mu^{-1/2}\left(\lambda_q^l\right)^{-1/2} - \left(\lambda_q^l\right)^{-1}, 0\right)$ is the power assigned to the stream $d_q^l[k]$. The constant μ is set to ensure that the constraint is active. In the OFDM case, the SNR is

$$\text{SNR}_q^l = 2\frac{\bar{p}_q^l\beta_q^l}{N_0},\ \ l = 1,...,S,\ \ q = 0,...,M-1. \tag{13}$$

Now the gain depends on $\left\{\beta_q^l\right\}$, which are the eigenvalues of $\mathbf{H}_q^H\mathbf{H}_q$. As a result, the per-stream powers are formulated as $\bar{p}_q^l = \max\left(\bar{\mu}^{-1/2}\left(\beta_q^l\right)^{-1/2} - \left(\beta_q^l\right)^{-1}, 0\right)$. Note that the noise power in (13) is not halved because in OFDM systems the processing is done over the complex field. The value 2 in the numerator indicates that $\left\{d_q^l[k]\right\}$ correspond to either real or imaginary parts of QAM symbols.

3.1. Real vs. complex processing

The real processing comes naturally to FBMC due to the non-circularity feature exhibited by the OQAM symbols. To determine if the proposed solution may remain competitive with the complex counterpart it is mandatory to know how (12) and (13) compare, which ultimately depends on the eigenvalues. To this end, let $\left\{\lambda_q^l\right\}$, $\left\{\mathbf{u}_q^l\right\}$ be respectively the non-zero eigenvalues and the corresponding eigenvectors of matrix $\bar{\mathbf{H}}_q^T\bar{\mathbf{H}}_q$. The eigenvalues are sorted in descending order, i.e. $\lambda_q^1 > ... > \lambda_q^{N_R}$. It is important to remark that we focus on the case that $N_T \geq N_R$. Furthermore, we assume that $\text{rank}(\mathbf{H}_q^H\mathbf{H}_q) = \text{rank}(\bar{\mathbf{H}}_q^T\bar{\mathbf{H}}_q) = N_R$. Regarding the OFDM counterpart, the non-zero eigenvalues of matrix $\mathbf{H}_q^H\mathbf{H}_q$ are collected in this set $\left\{\beta_q^1, ..., \beta_q^{N_R}\right\}$. It is worth noticing that the eigenvalues of $\mathbf{C}_q = \mathbf{F}_q^T\mathbf{F}_q$, where

$$\mathbf{F}_q = \begin{bmatrix} \Re(\mathbf{H}_q) & -\Im(\mathbf{H}_q) \\ \Im(\mathbf{H}_q) & \Re(\mathbf{H}_q) \end{bmatrix} = \begin{bmatrix} \mathbf{H}_{q,e}\mathbf{P} \\ \mathbf{H}_{q,e} \end{bmatrix}, \tag{14}$$

are also given by $\left\{\beta_q^l\right\}$ but with multiplicity equal to two. Hence, the eigenvalue β_q^l is associated to the eigenvectors $\mathbf{c}_q^l$ and $\bar{\mathbf{c}}_q^l$. Another interesting results is that $\mathbf{C}_q = \mathbf{H}_{q,e}^T\mathbf{H}_{q,e} + \mathbf{P}^T\mathbf{H}_{q,e}^T\mathbf{H}_{q,e}\mathbf{P}$, which implies that any column of $\mathbf{C}_q$ is a linear combination of these $2N_R$ column-vectors $\left[\mathbf{V}_{q,1}\ \ \mathbf{P}^T\mathbf{V}_{q,1}\right]$. If $\text{rank}(\mathbf{C}_q) = 2N_R$, then $\mathbf{C}_q$ and $\left[\mathbf{V}_{q,1}\ \ \mathbf{P}^T\mathbf{V}_{q,1}\right]$ span the same subsapce. Under this assumption, the null space of $\mathbf{C}_q$ is orthogonal to the space generated by the columns of $\mathbf{V}_{q,1}$, ($\text{null}(\mathbf{C}_q)\perp\text{span}(\mathbf{V}_{q,1})$). Defining $\mathbf{V}_q = [\mathbf{V}_{q,1}\mathbf{V}_{q,0}]$, then

$$\mathbf{n}^T\mathbf{s} = \mathbf{n}^T\mathbf{V}_q\mathbf{V}_q^T\mathbf{s} = \mathbf{n}^T\mathbf{V}_{q,0}\mathbf{V}_{q,0}^T\mathbf{s} = 0 \tag{15}$$

if $\mathbf{n} \in \text{null}(\mathbf{C}_q)$ and $\mathbf{s} \in \text{span}(\mathbf{C}_q)$. Since $\mathbf{V}_{q,0}^T\mathbf{C}_q\mathbf{V}_{q,0} = \bar{\mathbf{H}}_q^T\bar{\mathbf{H}}_q$, the eigenvectors $\left\{\mathbf{u}_q^l\right\}$ can be expressed as a linear combination of $\left\{\mathbf{V}_{q,0}^T\mathbf{c}_q^1, \mathbf{V}_{q,0}^T\bar{\mathbf{c}}_q^1, ..., \mathbf{V}_{q,0}^T\mathbf{c}_q^{N_R}, \mathbf{V}_{q,0}^T\bar{\mathbf{c}}_q^{N_R}\right\}$. Knowing that $\text{span}(\mathbf{C}_q) = \text{span}\left(\left[\mathbf{c}_q^1, \bar{\mathbf{c}}_q^1, ..., \mathbf{c}_q^{N_R}, \bar{\mathbf{c}}_q^{N_R}\right]\right)$, (15) becomes $\mathbf{n}^T\mathbf{V}_{q,0}\mathbf{u}_q^l = 0$ if $\mathbf{n} \in \text{null}(\mathbf{C}_q)$. As a result, the N_R unitary vectors given by $\mathbf{e}_q^l = \mathbf{V}_{q,0}\mathbf{u}_q^l$ satisfy: $\mathbf{e}_q^l \in \text{span}(\mathbf{C}_q)$. With the emphasis of the cases $l = 1$ and $l = N_R$, we obtain these inequalities

$$\begin{aligned} \beta_q^1 &= \max_{\mathbf{c}\in\text{span}(\mathbf{C}_q),\|\mathbf{c}\|_2=1} \mathbf{c}^T\mathbf{C}_q\mathbf{c} \geq \left(\mathbf{e}_q^1\right)^T\mathbf{C}_q\mathbf{e}_q^1 = \lambda_q^1 \\ \beta_q^{N_R} &= \min_{\mathbf{c}\in\text{span}(\mathbf{C}_q),\|\mathbf{c}\|_2=1} \mathbf{c}^T\mathbf{C}_q\mathbf{c} \leq \left(\mathbf{e}_q^{N_R}\right)^T\mathbf{C}_q\mathbf{e}_q^{N_R} = \lambda_q^{N_R}. \end{aligned} \tag{16}$$

In view of the results, we can state that the eigenvalues are less spread out when the proposed solution is applied. Hence,

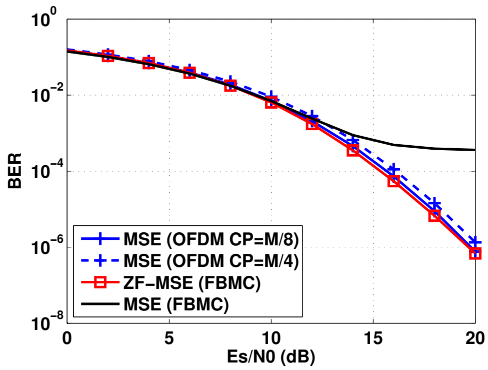

Fig. 1. BER vs. Es/N0 over a 2x4 MIMO channel.

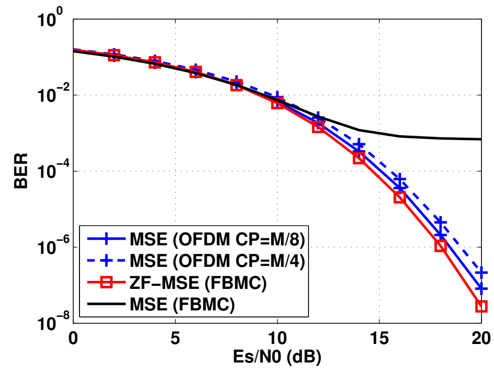

Fig. 2. BER vs. Es/N0 over a 4x8 MIMO channel.

the complex design will outperform the real one when $S = 1$ because $\beta_q^1 \geq \lambda_q^1$ and, therefore, the SINR of (12) will be always lower than that of (13). By contrast, if $S = N_R \leq N_T$ we cannot predict which design will give the best performance because at least in one spatial subchannel the real design achieves the highest gain, as it is demonstrated in (16).

4. NUMERICAL RESULTS

The simulations conducted in this Section aim at comparing the proposed MIMO technique with the solution that minimizes the sum MSE [9]. To differentiate when the technique is implemented in OFDM or FBMC, as [3] proposes, we use the acronyms MSE (OFDM) and MSE (FBMC), respectively. The proposed solution is based on the ZF condition, thus we name it ZF-MSE (FBMC). As we mention in the introduction, the robustness against synchronization errors is an aspect that may favour the implementation of FBMC over OFDM. In any case we evaluate the OFDM modulation scheme since the comparison is still interesting.

As for the system parameters the 10MHz bandwidth are divided into $M = 1024$ carriers, which $M_a = 720$ are used to carry symbols. Since the FBMC modulation allows us to better control the out-of-band radiation, the bands that remain silent are reduced. This translates to the utilization of $M_a = 756$ carriers to convey data, [10]. The sampling frequency is set to 11.2MHz and the symbols are drawn from the 16QAM scheme, which means that the real symbols multiplexed in the FBMC case are 4PAM. Finally the propagation conditions obey the ITU Vehicular A channel model.

The numerical results depicted in Fig. 1 and Fig. 2 show the BER against the average energy symbol to noise ratio (Es/N0), which is defined as $Es/N_0 = \frac{M+CP}{M}\frac{2P_T}{MN_0}$. In the FBMC case $CP = 0$. Based on the analysis carried out in Section 3.1 we focus on the configurations where this relation is satisfied: $S = N_R \leq N_T$. Especially interesting is the case of Fig. 1 where $S = 2$ because we have proven that $\lambda_q^1 \leq \beta_q^1$ and $\lambda_q^2 \geq \beta_q^2$. In this sense, Fig. 1 confirms that the loss in the first subchannel is compensated by the gain of the second subchannel. Note also that a short CP is preferable since less power is wasted. When the solution originally devised for OFDM is directly implemented in FBMC, the BER exhibits an error floor because the orthogonality is not restored and at low Es/N0 the residual interferences dominates over the noise [3]. The relative behaviour between techniques has not changed when the transmission is done over a 4x8 MIMO system. Again, the less spread out eigenvalues obtained in the proposed solution lead to a negligible degradation when compared to OFDM. However we have observed that this is not true in symmetric configurations where $S < N_R = N_T$.

Regarding the spectral efficiency, FBMC achieves $S3.3075$ bits/s/Hz, while OFDM takes $S2.52$ bits/s/Hz and $S2.8$ bits/s/Hz for CP=M/4 and CP=M/8, respectively.

5. CONCLUSIONS

To make progress in the MIMO applicability to FBMC we have devised a MIMO technique that allows us to spatially multiplex several streams on each subband. The proposed solution is able to deal with the channel frequency selectivity if the channel frequency response is flat at the subcarrier level. The analysis of the spatial subchannels in which the MIMO channel matrix is decoupled, reveals that the most interesting configurations satisfy this relation $S = N_R \leq N_T$. Simulation-based results have confirmed that the asymmetric configurations, i.e. $N_T > N_R$, succeed in providing similar BER results to OFDM but achieve a better spectral efficiency.

6. REFERENCES

[1] P. Siohan, C. Siclet, and N. Lacaille, “Analysis and design of OFDM/OQAM systems based on filterbank theory,” *IEEE Trans. on Signal Process.*, vol. 50, pp. 1170–1183, May 2002.

[2] B. Farhang-Boroujeny, “OFDM Versus Filter Bank

Multicarrier," *Signal Processing Magazine, IEEE*, vol. 28, no. 3, pp. 92 –112, may 2011.

[3] I. Estella, A. Pascual-Iserte, and M. Payaro, "OFDM and FBMC performance comparison for multistream MIMO systems," in *Future Network and Mobile Summit, 2010*, june 2010, pp. 1 –8.

[4] M. Caus and A. I. Perez-Neira, "Transmitter-Receiver Designs for Highly Frequency Selective Channels in MIMO FBMC Systems," *Signal Processing, IEEE Transactions on*, vol. 60, no. 12, pp. 6519 –6532, dec. 2012.

[5] M.G. Bellanger, "Specification and design of a prototype filter for filter bank based multicarrier transmission," Int. Conf. Acoustics, Speech, and Signal Processing, 2001, pp. 2417–2420.

[6] G.D. Golden, C.J. Foschini, R.A. Valenzuela, and P.W. Wolniansky, "Detection algorithm and initial laboratory results using V-BLAST space-time communication architecture," *Electronics Letters*, vol. 35, no. 1, pp. 14 –16, jan 1999.

[7] C.B. Peel, B.M. Hochwald, and A.L. Swindlehurst, "A vector-perturbation technique for near-capacity multiantenna multiuser communication-part I: channel inversion and regularization," *Communications, IEEE Transactions on*, vol. 53, no. 1, pp. 195 – 202, jan. 2005.

[8] R.F.H. Fischer, C. Windpassinger, A. Lampe, and J.B. Huber, "Space-Time Transmission using Tomlinson-Harashima Precoding," in *4th Int. ITG Conf.*, 2002, pp. 139–147.

[9] D.P. Palomar, J.M. Cioffi, and M.A. Lagunas, "Joint Tx-Rx beamforming design for multicarrier MIMO channels: a unified framework for convex optimization," *Signal Processing, IEEE Transactions on*, vol. 51, no. 9, pp. 2381 – 2401, sept. 2003.

[10] Qing Bai, N. Passas, and J.A. Nossek, "Scheduling and resource allocation in OFDM and FBMC systems: An interactive approach and performance comparison," in *Wireless Conference (EW), 2010 European*, april 2010, pp. 1042 –1050.